

## Predictive Numerical Simulation of ELMy H-mode Discharges for the KSTAR Tokamak

Ki Min Kim, Hyun Sun Han, Jin Myung Park, and Sang Hee Hong

*Department of Nuclear Engineering, Seoul National University, Seoul, Korea*

### Introduction

ELMs (Edge Localized Modes) in the tokamak have strong effects on its divertor conditions with a rapid increase in heat flux, and the pedestal parameters related to ELMs can work as constraints which impact the tokamak edge conditions to determine global confinements [1]. Therefore, a comprehensive understanding of the relations among ELM phenomena, pedestal parameters, and divertor heat conditions is essential for advanced tokamak operations like H-mode discharges. In this paper, the effects of ELMs on divertor heat flux and edge pedestal parameters are found by an integrated core-edge transport simulation for the KSTAR (Korea Superconducting Tokamak Advanced Research) tokamak [2].

### Numerical model and simulation results

Predictive numerical simulations of ELMy H-mode discharges are carried out for the KSTAR tokamak using an integrated plasma transport code, which has been recently developed in the authors' laboratory for a simultaneous treatment of core, edge pedestal, and scrape-off layer (SOL) regions of the tokamak [3]. In this integrated modelling, ELMs are supposed to be triggered by ballooning and peeling modes as expressed by the following equations [4, 5]:

$$\alpha_{mhd} \equiv -\frac{2\mu_0 R q^2}{\epsilon B^2} \left( \frac{dp}{dr} \right) > \alpha_{cr} = 0.4s \left( 1 + \kappa_{95}^2 (1 + 5\delta_{95}^2) \right)$$

$$\sqrt{1 - 4D_M} < C_k \left[ 1 + \frac{1}{\pi q'} \oint \frac{J_{\parallel} B}{R B_p^3} dl \right]$$

Here,  $J_{\parallel}$  is the current density parallel to the magnetic field  $B$ , and  $D_M$  is the Mercier coefficient which is proportional to pressure gradient included in the ballooning criterion. The above equations imply that ballooning mode and peeling mode are driven by pressure gradient and current density, respectively. However, the two triggering mechanisms are complicatedly linked, because pressure gradient could stabilize peeling

mode by increasing threshold, and also destabilize peeling mode by inducing edge current [6, 7, 8].

In the present simulation, neutral beam injection is applied as an external heating method, and the L-mode plasma is assumed to transit to an H-mode by the  $\mathbf{E} \times \mathbf{B}$  flow shear suppression of the edge transport with a rapid decrease in the released power across the separatrix. After the transition, edge transport coefficients are reduced to describe an enhanced pressure gradient at the pedestal and maintained until pedestal parameters reach the critical values limited by ballooning and peeling criteria. At the threshold, the ELM crash appears and the transport coefficients at the pedestal are increased to 100 times the neoclassical levels at the top of the pedestal to imitate the large energy and particle losses observed between neighboring ELMs.

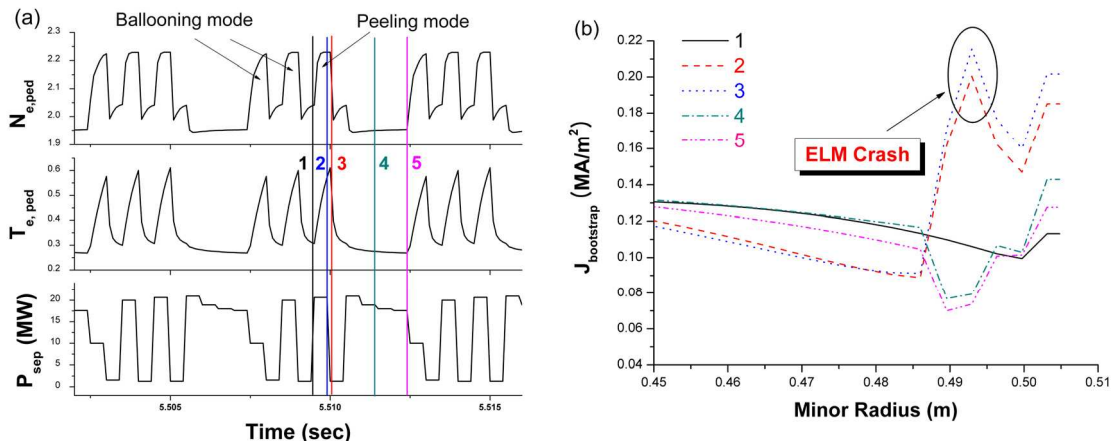


**Fig. 1** (a) Time trace of plasma density, temperature at the edge pedestal, and released power across the separatrix. ELM crashes by ballooning mode and peeling mode are observed by turns. (b) Radial profiles of bootstrap current densities during ELM crash triggered by peeling mode ( $P_{NBI}=8$  MW,  $I_P=2$  MA,  $n_{ave}=3.3 \times 10^{19}/m^3$ )

Figure 1 (a) shows that the pedestal density and temperature rapidly decrease by the ELM crashes and oscillate in a relatively constant frequency, but the total power crossing the separatrix increases with the released plasma particles. Different form of individual ELM crash is due to the coupling effect between ballooning and peeling modes. Because the growth of the pressure gradient leads a bootstrap current buildup which reduces the pressure gradient oppositely, the individual crash does not show a fixed wave form. However, one cycle of ELMs triggered by the coupled peeling-ballooning mode shows a uniform oscillating form.

Radial profile evolutions of bootstrap currents before and after one ELM crash

triggered by peeling mode are presented in Fig. 1. (b). Since the pressure gradient leads the buildup of bootstrap current in the edge region to make peeling mode unstable, the time evolution of bootstrap current is in step with ELM crashes triggered by peeling mode. On the other hand, bootstrap currents have stabilizing effects on ballooning criterion; the current profile at the edge region shows a complex behavior during coupled peeling-ballooning modes.

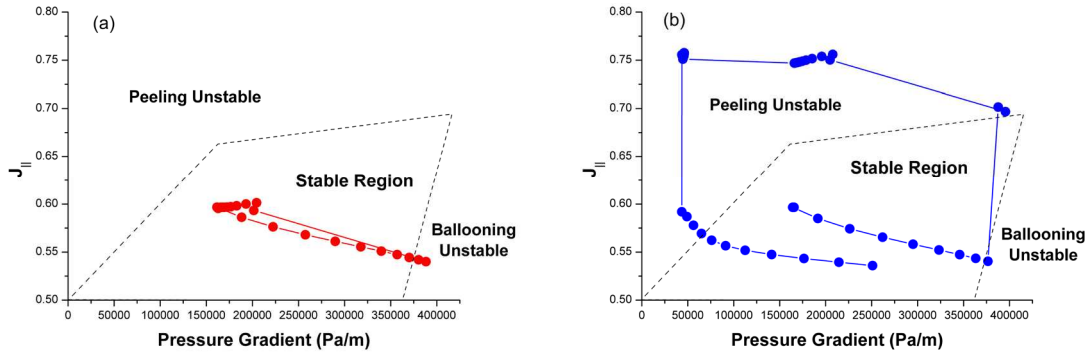


**Fig. 2** Stability diagrams for a peeling-ballooning mode. Edge current density vs. pressure gradient at the edge pedestal: (a) ballooning mode and (b) peeling mode. ( $P_{NBI}=8$  MW,  $I_P=2$  MA,  $n_{ave}=3.3 \times 10^{19}/m^3$ )

Figure 2 presents the stability diagrams which describe the relations between current density and pressure gradient at the pedestal for ballooning mode and peeling mode, separately. In case of ballooning mode, the pressure gradient increases with transport barrier and rapidly decreases at the critical pressure gradient, but the plasma current density does not show a considerable change. On the other hand, in case of peeling mode, the pedestal current density rapidly increases just below the critical pressure gradient due to the bootstrap current buildup by the rapid pressure gradient and moves the pedestal condition to an unstable region for the peeling mode criterion.

Since the ELM crashes triggered by both ballooning and peeling modes accompany energy release to the SOL region, heat fluxes onto the divertor plates show rapid increases by ELM crashes and repeat the buildup and relaxation processes keeping pace with pedestal parameters as shown in Fig. 3. The oscillations of heat flux onto the divertor plates naturally show the same tendencies with pedestal parameters. According to the simulation results, the maximum heat flux due to ELM crashes exceeds about  $12$  MW/m<sup>2</sup>, and increases with the neutral beam heating power, which means that ELM crashes have intolerable effects on the divertor modules, and therefore adequate controls of divertor conditions are needed for advanced tokamak experiments targeted by the KSTAR

project.

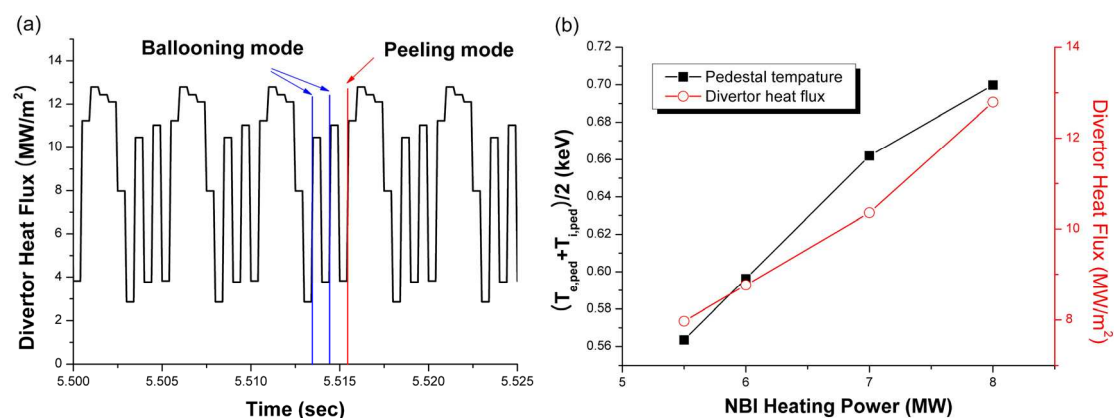


**Fig. 3** (a) Time trace of dumped heat flux on the divertor plate ( $P_{NBI}=8$  MW,  $I_P=2$  MA,  $n_{ave}=3.3\times 10^{19}/m^3$ ), and (b) scales of pedestal temperature and maximum heat flux with NBI heating power

## Conclusion

The numerical simulation results demonstrate that both ballooning mode and peeling mode can be sources of ELMs and limit the pedestal conditions. Especially, the evolution of edge current density, which depends on bootstrap current and pressure gradient at the pedestal, has different effects on pedestal parameters. Released powers by ELMs and divertor heat fluxes are predicted to lead intolerable heat sparks to the target plates, which could degrade tokamak confinement and cause a re-transition to the L-mode. For the more accurate estimation of divertor heat flux and pedestal parameters, another model for ELMs including more rigorous MHD effects are required. An integrated transport model which considers the plasma evolution with MHD stability analysis at every time step during ELMs would give more reliable insights into ELM phenomena.

## References

- [1] H. Zohm, Plasma Phys. Control. Fusion **38**, 105 (1996)
- [2] G. S. Lee, *et al.*, Nucl. Fusion **40**, 575 (2000)
- [3] J. M. Park, *et al.*, Bullet. Am. Phys. Soc. **48**, 346 (2003)
- [4] H. R. Wilson, *et al.*, Nucl. Fusion **40**, 713 (2000)
- [5] T. Onjun, *et al.*, Phys. Plasma **12**, 012506 (2005)
- [6] M. Bécoulet, *et al.*, Plasma Phys. Control. Fusion **45**, A93 (2003)
- [7] A. Y. Pankin, *et al.*, Plasma Phys. Control. Fusion **47**, 483 (2005)
- [8] J. S. Lönnroth, *et al.*, Plasma Phys. Control. Fusion **46**, 1197 (2004)